J. Anat. (2001) **199**, pp. 449–456, with 4 figures Printed in the United Kingdom

Changes in aponeurotic dimensions upon muscle shortening: in vivo observations in man

CONSTANTINOS N. MAGANARIS, YASUO KAWAKAMI AND TETSUO FUKUNAGA

University of Tokyo, Komaba, Department of Life Sciences, Komaba 3-8-1, Meguro, Tokyo 153-8902, Japan

(*Accepted 11 April 2001*)

ABSTRACT

Aponeurotic deformation measurements have traditionally been taken by loading dissected muscles; thus the values obtained may not reflect in vivo function. In the present study, we estimated dimensional changes in the central aponeurosis of the intact human tibialis anterior muscle upon loading induced by muscle contraction. Measurements were taken in seven males, and involved real-time ultrasound scanning of the tibialis anterior muscle at 30° of plantarflexion at rest and during isometric dorsiflexion maximum voluntary contraction (MVC). At each contraction state, the length of the aponeurosis, the width along its length, and its area were estimated from sagittal-plane and axial-plane sonographs. In the transition from rest to MVC, the length of the aponeurosis increased by 7% ($P < 0.05$), its width increased by up to 21% ($P < 0.05$), and its area increased by 17% ($P < 0.05$). These results indicate that the in vivo tibialis anterior aponeurosis behaves as a compliant material upon active muscle shortening. The methodology employed allows cross-sectional and longitudinal design investigations, circumventing the problems associated with epimysial removal under in vitro experimental conditions.

Key words: Tendinous tissue; elasticity; muscle contraction; ultrasound.

INTRODUCTION

The intramuscular portion of tendon in which the muscle fibres insert is referred to as the aponeurosis. Like the extramuscular tendon portion, the aponeurosis is a collagenous structure and deforms upon load application in a predictable nonlinear manner (Huijing & Ettema, 1988/1989; Ettema & Huijing, 1989; Lieber et al. 1991; Trestik & Lieber, 1993; Zuurbier et al. 1994; Scott & Loeb, 1995; Maganaris & Paul, 2000*a*).

The extensibility of aponeuroses when loaded by contractile muscle forces is an important input parameter in modelling-based studies of muscle pressure, architecture and performance (Huijing & Woittiez, 1985; Bobbert et al. 1986; Zuurbier & Huijing, 1992; van Leeuwen & Spoor, 1993, 1996). In vitro experiments have shown that aponeuroses may deform by up to 10% longitudinally and 6% transversally during muscle contraction (Huijing & Ettema, 1988/1989; Ettema & Huijing, 1989; Lieber et al. 1991; Trestik & Lieber, 1993; Zuurbier et al. 1994; Scott & Loeb, 1995; van Donkelaar et al. 1999). Reference, however, to these values when inferring in vivo function should be treated with caution. Under in vitro experimental conditions, aponeurotic deformations have been obtained from displacement recording of markers inserted in the aponeurosis after removing the epimysium. Epimysial release, however, alters (1) the intramuscular pressure and (2) the force exerted by the muscle during contraction (Mozan & Keagy, 1969; Garfin et al. 1981). These effects indicate that the epimysium may affect the contractile force transmitted in the aponeurosis, and thus the epimysium should be intact when examining aponeurotic deformations under physiological conditions.

Realtime ultrasonography allows scanning of aponeurotic tissue in intact human muscles (Kawakami et al. 1993; Narici et al. 1996; Maganaris et al. 1998; Maganaris & Paul, 2000*a*, *b*). In the present ex-

Correspondence to Dr C. Maganaris, Manchester Metropolitan University, Active Life Span Research, Alsager Campus, Stoke-on-Trent, ST7 2HL, UK. Tel.: +161 247 5428; fax: +161 247 6375; e-mail: C.N.Maganaris@mmu.ac.uk

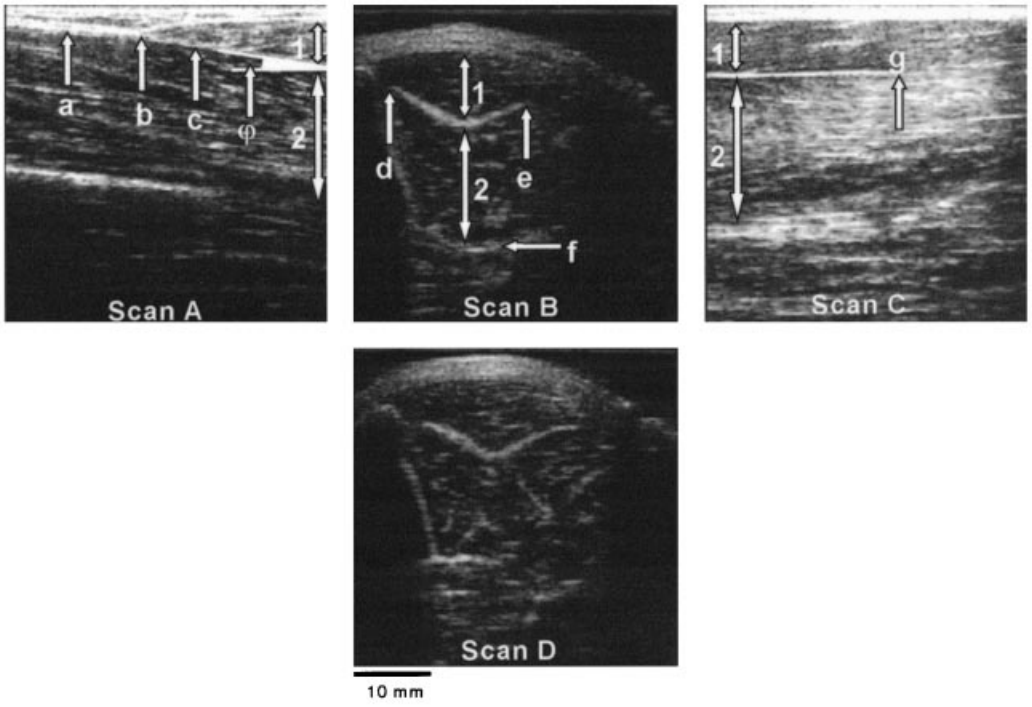

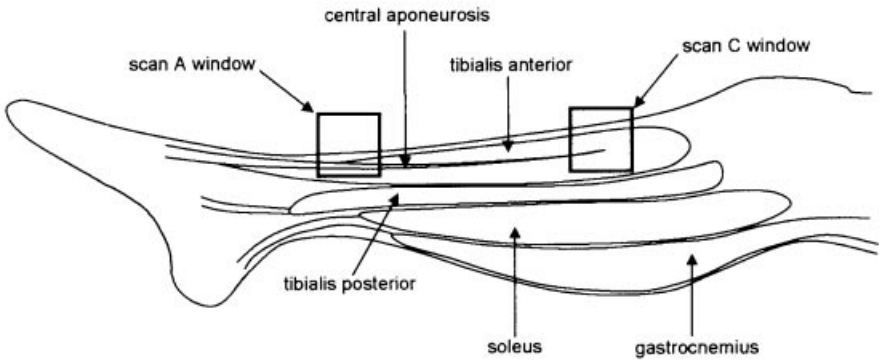

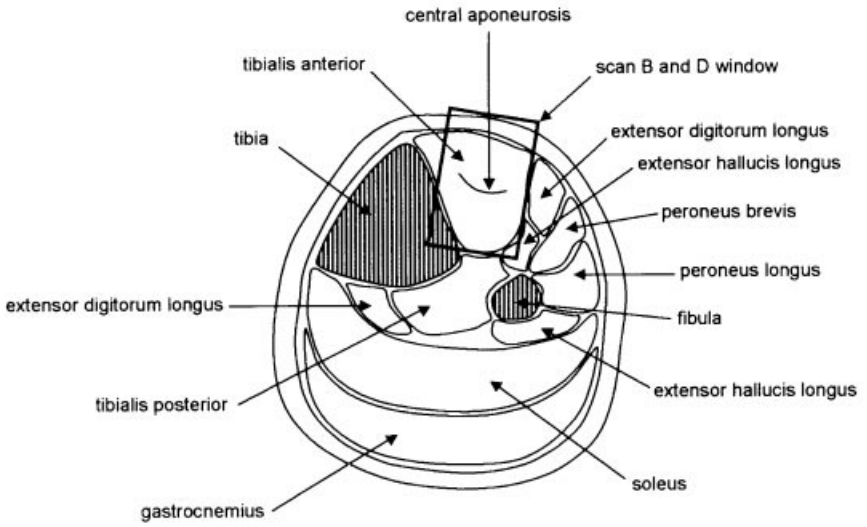

Fig. 1. Top: Typical sonographs over the TA muscle of the right leg at 30° of plantarflexion. Scans A, B and C were recorded at rest, and scan D was recorded during MVC. The probe was placed in the midsagittal plane for scans A and C, and in the axial plane for scans B and D. Scan A was taken 20 cm above the level of malleoli, scan C was taken 17 cm proximal to the myotendinous junction, and scans B and D were taken 8 cm proximal to the myotendinous junction. a, TA tendon; b, myotendinous junction; c, central aponeurosis; φ, angle of

periment, we used this technique to quantify aponeurotic deformations upon active muscle shortening.

METHODS

Seven healthy male volunteers (average—mean ± SD—age, height, body mass and lower leg length, 23 ± 4 y, 172 ± 3 cm, 73.5 ± 3 kg and 39.5 ± 2 cm, respectively) gave their written consent to participate in the study. The experiment was approved by the institutional ethics committee. We examined the central aponeurosis of the human tibialis anterior (TA) muscle. The TA central aponeurosis is a 3-dimensional (3D) structure that continues from the extramuscular tendon and extends into the muscle belly dividing a major portion of the whole muscular length into 2 unipennate halves, one above and the other below the aponeurosis. In the present study, we measured the length and the width of the aponeurosis. The length corresponds to the distance between proximal and distal ends; the width corresponds to the length of the curvature of the aponeurosis between medial and lateral edges.

Measurements were taken in the prone position on the bench of an isokinetic dynamometer (Lido Active, Loredan Biomedical, Davis, CA), having the knee of the tested leg (the right leg in all subjects) flexed at 90°, and the ankle flexed at 30° of plantarflexion (0°: the sole of the foot perpendicular to the shank). At this ankle angle, the dorsum of the foot is aligned with the shank and the TA muscle-tendon unit operates over a straight line. Velcro straps around the foot and a mechanical stop below the knee were used to secure the lower extremity at the position studied. The TA aponeurosis' distal end in the myotendinous junction (~ 20 cm above the level of malleoli) and the proximal end of the aponeurosis (~ 36 cm above the level of malleoli) were first identified in the midsagittal plane of the TA muscle at rest using a 7.5 MHz linear B-mode ultrasound probe (Esaote Biomedica, Florence; width and depth resolutions, 1 and 0.62 mm, respectively). The exact positions of the aponeurosis' proximal and distal end echoes were then located from axial-plane scans taken in the above regions, and marked over the skin. Consecutive axial-plane scans were then taken from the aponeurosis' distal end to the aponeurosis' proximal end every 1 cm. The same procedure was repeated during isometric dorsiflexion maximum voluntary contraction (MVC). Contractions were separated by 1 min and repeated until the dorsiflexion moments recorded were within ± 5% of the dorsiflexion moment elicited upon MVC in a familiarisation trial 2–3 d earlier. Data were collected in a randomised order for contraction state.

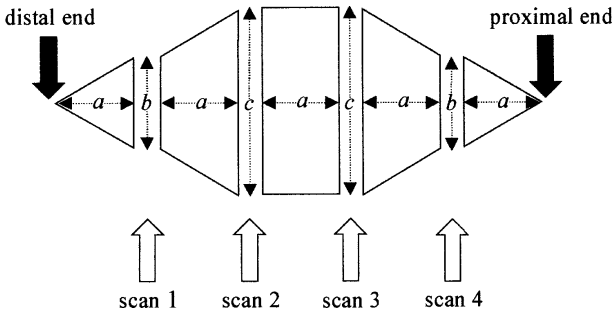

Fig. 2. Example of dimensional measurements in the TA aponeurosis. The aponeurosis lies in the frontal plane and the white arrows indicate levels at which axial-plane sonographs were recorded to obtain width data. In the example shown the area between the aponeurosis' distal end and scan 1 (and that between scan 4 and the aponeurosis' proximal end) is $1/2 \cdot b \cdot a$, that between scans 1 and 2 (and scans 3 and 4) is $1/2 \cdot (b+c) \cdot a$, and that between scans 2 and 3 is $a \cdot c$. The aponeurosis' length is $5 \cdot a$, and its width is b in scans 1 and 4, and c in scans 2 and 3.

The length of a straight line over the skin between the aponeurosis' proximal and distal end echoes was considered as the aponeurosis' length. The aponeurosis was almost parallel to the skin along the whole aponeurotic length, apart from the myotendinous junction region where the aponeurosis approached the skin at an angle of ~ 8° (Fig. 1). Trigonometry-based calculations indicated that assuming the angle between the aponeurosis and the skin to be 0° would result in an underestimation of the actual entire aponeurotic length by ~ 1%. Thus we considered that aponeurotic length measurements over a straight line were realistic. In each one of the axial-plane scans taken, the aponeurotic width was identified and digitised (NIH Image, National Institute of Health, Bethesda, MD) following its curved path from the medial edge to the lateral edge (Fig. 1). The aponeurosis' area between every 2 consecutive axial-plane scans was calculated treating the interscan aponeurotic shape as a triangle, trapezoid or parallelogram, depending on the width of the aponeurosis in each scan (Fig. 2). On most of the occasions, the interscan distance in the 2 most proximal axial-plane sonographs was adjusted in less than 1 cm, and

aponeurotic orientation relative to the horizontal (~ 8°); d, aponeurotic medial edge; e, aponeurotic lateral edge; f, surrounding epimysium; g, aponeurotic proximal end; 1, superficial unipennate half of the TA muscle; 2, deep unipennate half of the TA muscle. The superficial and deep aponeuroses of the TA muscle lie at the top and bottom, respectively, of the muscle cross-section as bordered by the epimysium shown in scans B and D (see also Fig. 4). Bottom: Schematic representations of the shank in the sagittal and axial planes.

this was taken into account in the corresponding area calculations. The whole area of the aponeurosis was estimated by summing up all interscan areas (Fig. 2).

Statistics

Values are presented as means ± S.D. Student's paired *t*-test was used to test differences in aponeurotic length, width in a given scan, and area between rest and MVC. Statistical difference was set at a level of $P < 0.05$. A statistical power analysis indicated that 6 subjects would suffice to reject a false null hypothesis in the study.

RESULTS

All aponeurotic dimensions examined increased in the transition from rest to MVC (Fig. 3). The aponeurosis' length increased from 165 ± 6 to 177 ± 6 mm (7%, $P < 0.05$; Fig. 3*a*). The aponeurotic width increased by between 8% (from 8.7 ± 1 to 9.4 ± 1.2 mm, $P > 0.05$; last scan before the proximal end of the aponeurosis) and 21% (20.4 ± 2–24.4 ± 2 mm, $P < 0.05$; 7th scan after the distal end of the aponeurosis; Fig. 3*b*). The entire area of the aponeurosis increased from 2327 ± 197 to 2715 ± 202 mm^2 (17%, $P < 0.05$; Fig. 3*c*).

Accuracy and reproducibility of ultrasound scanning

Direct measurements on cadaveric material have previously shown that ultrasonography locates very accurately intramuscular connective tissue (Kawakami et al. 1993; Narici et al. 1996). Inter-and intraobserver variation values of ultrasound-based measurements of aponeurotic length at rest and during MVC have been confirmed to range between 2 and 4% (Maganaris & Paul, 2000*a*, *b*). In the present study we also assessed the repeatability of measuring aponeurotic width. Repeated scanning (14 times over 7 consecutive days) of the TA aponeurosis' width 2, 8 and 14 cm proximal to the myotendinous junction resulted in coefficient of variation values in the range of 2 to 4% at rest and 2 to 6% during MVC. Four different researchers scanned the TA aponeurosis' width 8 cm proximal to the myotendinous junction, and the resulted coefficients of variation were 3% at rest and 8% during MVC.

It must be emphasised that any contraction-induced shift of the ultrasound probe on the skin would result in artifactual measurements of aponeurotic dimensions. By using echoabsorptive markers glued on the skin, we have previously confirmed the constancy in the probe position during isometric contractions (Maganaris & Paul, 2000*a*, *b*).

DISCUSSION

In the present paper, we present ultrasound-based data of aponeurotic deformation upon loading induced by muscle contraction. In contrast with previous studies, in this experiment deformations were obtained under in vivo conditions.

The length of the aponeurosis increased in the transition from rest to MVC. This effect is associated with activation of contractile tissue attached to the aponeurosis. During muscle contraction, force is exerted along the direction of muscle fibres (Fig. 4). The effective component of contractile force transmitted along the aponeurosis, pulls the aponeurosis proximally and causes a longitudinal deformation with size proportional to the amount of in-parallel contractile material in the muscle or the level of volitional force elicited (Maganaris & Paul, 2000*a*, *b*).

Aponeurotic elongation upon contraction could also be associated with changes in the geometry of muscle fibres. During contraction the muscle fibres shorten. To maintain their volume constant, their cross-sectional area must increase. Accommodation of this increase in pennate muscles can be accomplished by increasing (1) the pennation angle, and (2) the attachment area of the fibre in the aponeurosis (Willems & Huijing, 1994, Scott & Loeb, 1995). An increase in the anteroposterior diameter of the fibre attachment area (i.e. the diameter of the attachment area in the sagittal plane) would lengthen the aponeurosis, while an increase in the mediolateral diameter of the fibre attachment area (i.e. the diameter of the attachment area in the axial plane) would widen the aponeurosis. The latter effect may account for the width changes obtained in our experiment.

Fibre bulging should also be considered when examining contraction-induced changes in aponeurotic width. During muscle contraction, intramuscular pressure builds up resulting in fibre curvature (Otten, 1988; van Leeuwen & Spoor, 1993, 1996). The horizontal vector components of the forces acting along the curved fibres would deform the aponeurosis in the axial plane, increasing its width both medially and laterally (Fig. 4).

Our aponeurotic deformation estimates are in line with in vitro measurement-based results. Experiments on isolated aponeuroses subjected to loading equivalent to the force generating potential of the corresponding muscles have given longitudinal strain values in the range of 1 to 14%, and transverse strain

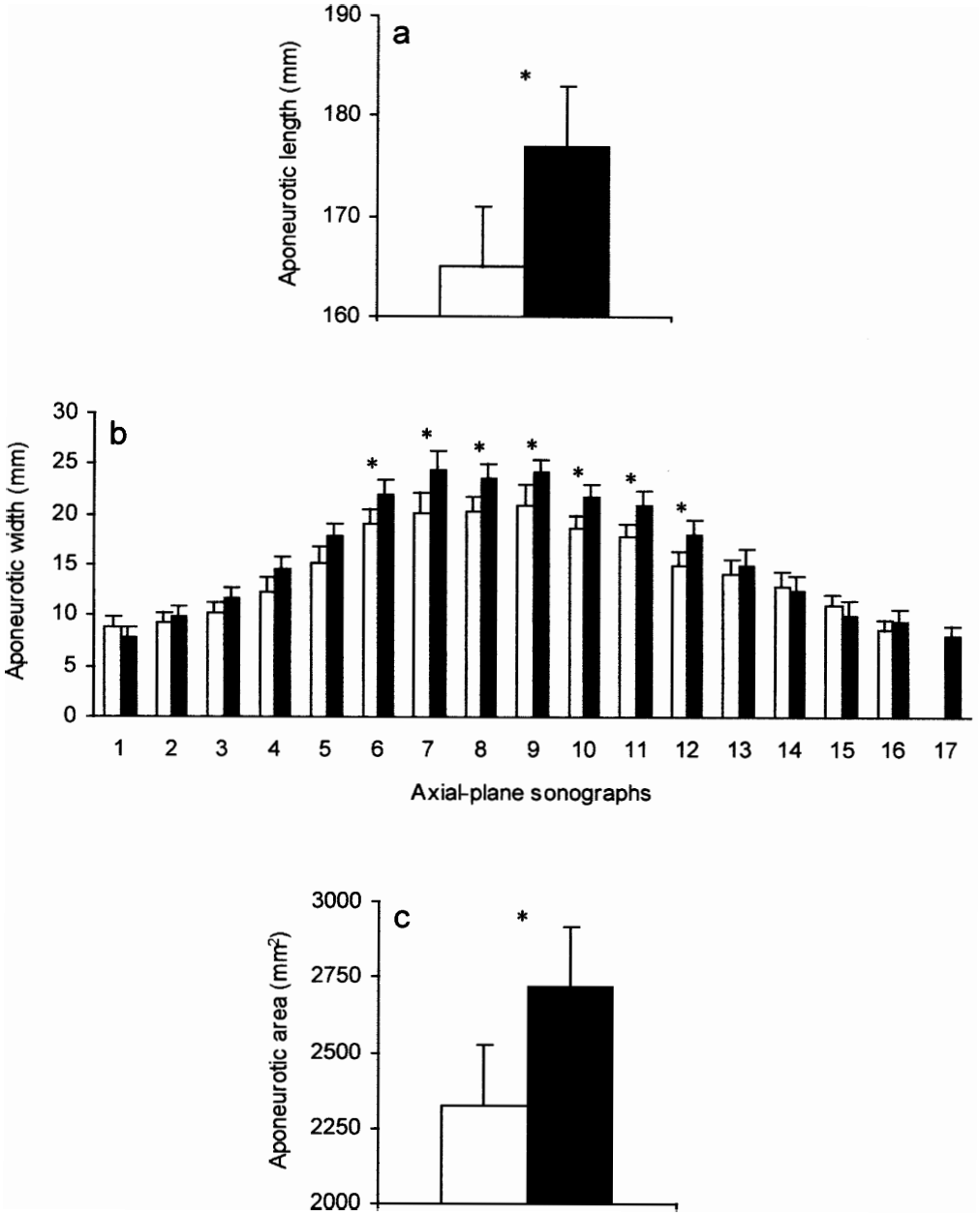

Fig. 3. In vivo measurements of length (*a*), width (*b*) and area (*c*) in the TA aponeurosis. White bars represent resting-state dimensions and black bars MVC-state dimensions. In graph *b*, sonograph 1 is the first scan after the distal end of the aponeurosis. The highest-number sonograph is the last scan before the proximal end of the aponeurosis. The interscan distance is 1 cm. Notice that the aponeurotic width decreases gradually from the central region of the length of the aponeurosis towards its proximal and distal ends, i.e. the aponeurosis has a leaf-like shape. In all graphs shown, data represent mean values and error bars S.D. values ($n = 7$). * indicates $P < 0.05$ between resting-state and MVC-state dimensions.

values of $\sim 6\%$ (Huijing & Ettema, 1988/1989; Ettema & Huijing, 1989; Lieber et al. 1991; Trestik & Lieber, 1993; Zuurbier et al. 1994; Scott & Loeb, 1995; van Donkelaar et al. 1999). The general consensus between experimental results, however, should be interpreted in the light of four important points.

(1) In contrast with in vitro experiments, where transverse deformations at a given width level have been obtained, in the present study we estimated axial-plane deformations from morphometrics of a given level image relative to a moving reference point (the distal end of the aponeurosis) between contraction states. Thus our estimates may not reflect increases in aponeurotic width over given aponeurotic lengths.

(2) In the present experiment the ankle was plantarflexed. This position was selected to attain a straight-line orientation between the origin and insertion of the TA muscle-tendon unit and eliminate artifactual aponeurotic deformations due to a retinaculum stretch upon dorsiflexion contraction (Magan-

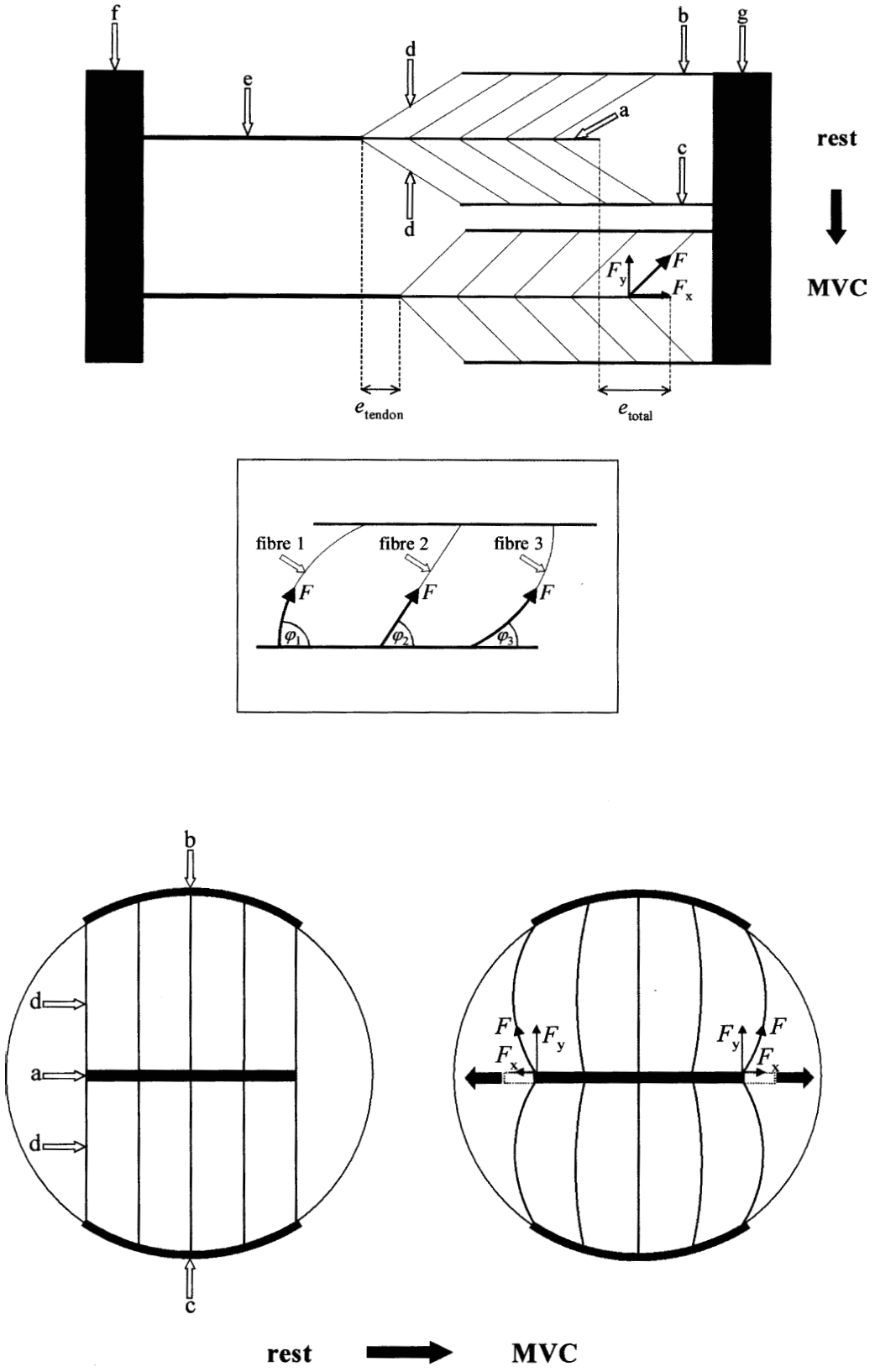

Fig. 4. Top: Sagittal-plane model of the TA muscle. Each unipennate half of the bipennate TA muscle is modelled as a parallelogram. a, central aponeurosis; b, superficial aponeurosis; c, deep aponeurosis; d, muscle fibres; e, tendon; f, distal end of the muscle-tendon unit; g, proximal end of the muscle-tendon unit; e_{tendon}, tendon elongation upon MVC; $e_{total,}$ tendon + aponeurosis elongation upon MVC. During MVC the fibres shorten and their pennation angle increases. F_x and F_y are the horizontal and vertical vector components, respectively, of the fibre force F during MVC. F_x acts along the aponeurosis and increases its length. In the inset bellow, the effect of fibre curvature on pennation angle is illustrated in the superficial unipennate half of the muscle. Fibre 1 lies in the muscle's distal region, fibre 2 lies in the

aris et al. 1999). Ankle plantarflexed positions at rest, however, may not correspond to dimensions reflecting 0% strain in the TA aponeurosis. Thus, our dimensional deformations may not represent accurate estimates of the TA aponeurosis' mechanical properties.

(3) The multiple measurements taken during MVC would be affected by the time-dependent properties of collagenous tissue. Thus, some creep would be expected and included in the deformations obtained.

(4) We obtained aponeurotic deformations with the muscle being surrounded by its epimysium. In in vitro experiments the epimysium has been removed to eliminate artifactual marker displacements (Zuurbier et al. 1994; Scott & Loeb, 1995; van Donkelaar et al. 1999). Epimysial release, however, reduces the pressure and the force generated in the muscle during contraction (Mozan & Keagy, 1969; Garfin et al. 1981). Both effects would reduce fibre curvature (Aratow et al. 1993; Maganaris et al. 1998). A decreased curvature in a pennate fibre would result in less force transmitted across the aponeurosis. Thus smaller changes in aponeurotic width would be obtained upon contraction with the epimysium removed (Fig. 4). The effect of a decreased pennate fibre curvature on aponeurotic length would depend on the length region examined. In the proximal region of the aponeurosis, where the fibres bulge in a concave pattern relative to the distal end of the aponeurosis, a decreased curvature would result in less force transmitted along the aponeurosis. Thus, smaller longitudinal deformations would be obtained upon contraction with the epimysium removed. In contrast, in the distal region of the aponeurosis, where the fibres bulge in a convex pattern relative to distal end of the aponeurosis, a decreased curvature would result in more force transmitted along the aponeurosis. Thus, larger longitudinal deformations would be obtained upon contraction with the epimysium removed (Fig. 4).

In conclusion, we showed that the resting-state dimensions of the in vivo human TA aponeurosis increase during muscle contraction. The noninvasive method employed in the study allows design of cross-sectional and longitudinal experimental protocols in intact human muscles.

ACKNOWLEDGEMENTS

This work was supported by a postdoctoral fellowship from the Japan Society for the Promotion of Science (JSPS).

REFERENCES

ARATOW M, BALLARD RE, CRENSHAW AG, STYF J, WATENPAUGH DE, KAHAN NJ et al. (1993) Intramuscular pressure and electromyography as indexes of force during isokinetic exercise. *Journal of Applied Physiology* **74**, 2634–2640.

BOBBERT MF, HUIJING PA, VAN INGEN SCHENAU GJ (1986) A model of human triceps surae muscle-tendon complex applied to jumping. *Journal of Biomechanics* **19**, 887–898.

ETTEMA GJC, HUIJING PA (1989) Properties of the tendinous structures and series elastic component of the EDL muscle-tendon complex of the rat. *Journal of Biomechanics* **22**, 1209–1215.

GARFIN SR, TIPTON CM, MUBARAK SJ, WOO SL-Y, HARGENS AR, AKESON WH (1981) Role of fascia in maintenance of muscle tension and pressure. *Journal of Applied Physiology* **51**, 317–320, 1981.

HUIJING PA, WOITTIEZ RD (1985) Notes on planimetric and three-dimensional muscle models. *Netherlands Journal of Zoology* **35**, 521–525.

HUIJING P A, ETTEMA GJC (1998/1989) Length-force characteristics of aponeurosis in passive muscle and during isometric and slow dynamic contractions of rat gastrocnemius muscle. *Acta Morphologica Neerlando-Scandinavica* **26**, 51–62.

KAWAKAMI Y, ABE T, FUKUNAGA T (1993) Muscle-fiber pennation angles are greater in hypertrophied than in normal muscles. *Journal of Applied Physiology* **74**, 2740–2744.

LIEBER RL, LEONARD ME, BROWN CG, TRESTIK CL (1991) Frog semitendinosis tendon load-strain and stress-strain properties during passive loading. *American Journal of Physiology* **261**, C86–C92.

MAGANARIS CN, BALTZOPOULOS V, SARGEANT AJ (1998) In vivo measurements of the triceps surae architecture in man: Implications for muscle function. *Journal of Physiology* **512**, 604–613.

MAGANARIS CN, BALTZOPOULOS V, SARGEANT AJ (1999) Changes in the tibialis anterior tendon moment arm from rest to maximum isometric dorsiflexion: In vivo observations in man. *Clinical Biomechanics* **14**, 661–666.

MAGANARIS CN, PAUL JP (2000*a*) Load-elongation characteristics of in vivo human tendon and aponeurosis. *Journal of Experimental Biology* **203**, 751–756.

MAGANARIS CN, PAUL JP (2000*b*) In vivo human tendinous tissue stretch upon maximum muscle force generation. *Journal of Biomechanics* **32**, 1453–1459.

MOZAN LC, KEAGY RB (1969) Muscle relationship in functional fascia—a preliminary study. *Clinical Ortopaedics* **67**, 225–230.

NARICI MV, BINZONI T, HILTBRAND E, FASEL J, TERRIER F, CERRETELLI P (1996) In vivo human gastrocnemius architecture with changing joint angle at rest and during graded isometric contraction. *Journal of Physiology* **496**, 287–297.

OTTEN E (1988) Concepts and models of functional architecture in skeletal muscle. *Exercise and Sports Science Reviews* **16**, 89–137.

muscle's central region, and fibre 3 lies in the muscle's proximal region (see also Otten, 1988; van Leeuwen & Spoor, 1992, 1996). Because $\varphi_1 > \varphi_2 > \varphi_3$, the effective contractile force transmitted along the aponeurosis decreases from proximal to distal regions. Contraction-effects on the superficial and deep aponeuroses of the muscle are not shown. Bottom: Axial-plane model of the TA muscle. a, central aponeurosis; b, superficial aponeurosis; c, deep aponeurosis; d, projected muscle fibres on the transverse plane. During MVC, peripheral fibres bulge in response to the high intramuscular pressure developed. F_x and F_y are the horizontal and vertical vector components, respectively, of the fibre force F during MVC. F_x acts across the aponeurosis and increases its width. Contraction-effects on the superficial and deep aponeuroses of the muscle are not shown.

SCOTT SH, LOEB GE (1995) Mechanical properties of aponeurosis and tendon of the cat soleus muscle during whole-muscle isometric contractions. *Journal of Morphology* **224**, 73–86.

TRESTIK CL, LIEBER RL (1993) Relation between Achilles tendon mechanical properties and gastrocnemius muscle function. *Journal of Biomechanical Engineering* **115**, 225–230.

VAN DONKELAAR CC, WILLEMS PJB, MUIJTJENS AMM, DROST MR (1999) Skeletal muscle transverse strain during isometric contraction at different lengths. *Journal of Biomechanics* **32**, 755–762.

VAN LEEUWEN JL, SPOOR CW (1993) Modelling the pressure and force equilibrium in unipennate muscles with in-line tendons. *Philosophical Transactions of the Royal Society of London B* **342**, 321–333.

VAN LEEUWEN JL, SPOOR CW (1996) A two-dimensional model for the prediction of muscle shape and intramuscular pressure. *European Journal of Morphology* **34**, 25–30.

WILLEMS MET, HUIJING PA (1994) Mechanical and geometrical properties of the rat semimembranosus lateralis muscle during isometric contractions. *Journal of Biomechanics* **27**, 1109–1118.

ZUURBIER CJ, HUIJING PA (1992) Influence of muscle geometry on shortening speed of fibre, aponeurosis and muscle. *Journal of Biomechanics* **25**, 1017–1026.

ZUURBIER CJ, EVERARD AJ, VAN DER WEES P, HUIJING PA (1994) Length-force characteristics of the aponeurosis in the passive and active muscle condition and in the isolated condition. *Journal of Biomechanics* **27**, 445–453.